Evaluation of Two Susceptibility-Weighted Sequences for Detection of Cerebral Microbleeds

Cheryl R McCreary[1,2], M Louis Lauzon[1,2], Saima Batool[1,2], Eric E Smith[1,2], and Richard Frayne[1,2]

[1]*Radiology and Clinical Neurosciences, Hotchkiss Brain Institute, University of Calgary, Calgary, Alberta, Canada,* [2]*Seaman Family MR Centre, Foothills Medical Centre, Calgary, Alberta, Canada*

Target Audience: Researchers, scientists, technicians, and clinicians interested in susceptibility imaging or evaluation of MR imaging sequences for detection of cerebral microbleeds or regions of low venous cerebral blood flow.

Purpose: In an ongoing prospective, longitudinal study on potential MR biomarkers of cognitive impairment in aging called Functional Assessment of Vascular Reactivity (FAVR), we have acquired and processed susceptibility-weighted images (SWI) based on the methods suggested by Haacke [1] to identify cerebral microbleeds (CMBs). More recently, we have also acquired quantitative susceptibility maps (QSM); a novel method that uses multi-echo spoiled gradient echo images [2] to quantify iron accumulation in addition to identification of CMBs. However, it is unknown whether a single echo from the multi-echo acquisition can be used to visually identify microbleeds with similar sensitivity as SWI. We compared the number and contrast of CMBs detected on SWI and similarly phase-filtered images generated from the sixth echo of the QSM (SWI_{6e}) dataset in a subset of participants to determine if the multi-echo sequence is equivalent to SWI for CMB detection and can replace SWI in FAVR.

Methods: SW and QSM data were acquired for 17 consecutive FAVR participants (Table 1) using a 3 T scanner (Discovery 750, GE Healthcare). For SW images, a 3D vascular time-of-flight spoiled gradient recalled echo (GRE) sequence was modified to save both real and imaginary images (TR=30 ms, TE=20 ms, flip=15°, rBW=±31.25 kHz, ASSET=2, TA= 4:48 min, FOV=25.6 mm, slice thickness=2 mm, acquisition matrix=256×256×72 reconstructed to 0.5×0.5×1.0 mm^3 voxels). For QSM images, a multi-echo 3D spoiled GRE sequence was modified to incorporate unipolar readout gradients, 3D flow compensation, and to save real and imaginary images (TR=min, 8 echoes, TE=min, inter-echo spacing= 3.3 ms, flip=20°, rBW=±42.67 kHz, ASSET=1, TA=4:10 min, FOV=25.6 mm, slice thickness=2 mm, acquisition matrix=192×192×72 reconstructed to 1.0×1.0×1.0 mm^3 voxels). Real and imaginary images from the SWI_{6e} data (at TE~20 ± 2 ms) were processed using the same method as SW processing. Each set of processed images was presented in a random order for review to a trained reader in order to identify CMBs. The number of detected CMBs and contrast of the each CMB within individuals was compared between SWI and SWI_{6e} images. The contrast, calculated as the difference between signal from manually drawn regions-of-interest (ROI) in the tissue surrounding a CMB and signal from a ROI within the CMB divided by the tissue signal, was performed for each subject. In the case where an individual had multiple CMBs, one CMB was randomly selected for analysis.

Results: One set of images was excluded from the analysis due to subject motion during acquisition. Sample SW and SWI_{6e} images are shown in Figure 1. CMBs were detected in 11/16 participants. Concordant numbers of CMBs were found in 5 of the 11 CMB-presenting participants. However, in 5/6 of the remaining cases, more CMBs were detected on SWI than SWI_{6e} (Table 2). The intra-class correlation coefficient between SWI and SWI_{6e} was 0.88. The mean contrast was significantly higher on SW images compared to SWI_{6e} [0.65 (standard deviation of 0.10) versus 0.45 (0.13), respectively; p<0.01, paired t-test].

Discussion: The discordance between SWI and SWI_{6e} may result from differences in contrast and resolution between methods. SWI had an in-plane reconstructed resolution of 0.5×0.5 mm^2 compared to 1.0×1.0 mm^2 for QSM. Vernooij *et al.* have shown that image resolution impacts detectability of CMBs. We chose a lower resolution for the SWI_{6e} acquisition for two reasons: first, to achieve a similar acquisition time to SWI and second, to manage the computational demands required for the phase unwrapping and deconvolution of the dipole moment used in QSM (not used in this study). We are working on modifying the QSM processing code to overcome this limitation.

Conclusion: SWI is currently implemented as the standard technique used at our site for several dementia research studies for identification of CMBs. While QSM has potential to provide additional quantitative information on brain iron accumulation, there may be some bias toward underestimating the number of CMBs in our implementation of QSM, which might be correctable with higher resolution QSM imaging.

References: 1. Haacke, EM, *et al.*, (2009) Am J Neuroradiol 30:19-30. 2. Li, J, *et al.*, (2012) MRM 68:1563-1569. 3. Vernooij, MW, *et al.*, (2008) Radiology 248:272-277.

Table 1. Participant Demographics

Mean Age (y; SD)	73.6 (7.9)
Female:Male	5:11
Diagnosis:	
Cerebral Amyloid Angiopathy	9
Mild Cognitive Impairment	4
Alzheimer's Disease	4

Table 2. Comparison of Cerebral microbleeds detected between SWI and SWI6e. Cases with discordant CMB detection are highlighted.

Subject	Diagnosis	SW image	6eQSM
S1	CAA	6	5
S2	MCI	2	2
S4	CAA	3	3
S5	CAA	2	1
S6	CAA	8	10
S7	CAA	6	3
S8	CAA	7	7
S9	AD	1	0
S15	CAA	2	0
S16	CAA	3	3
S17	CAA	5	5

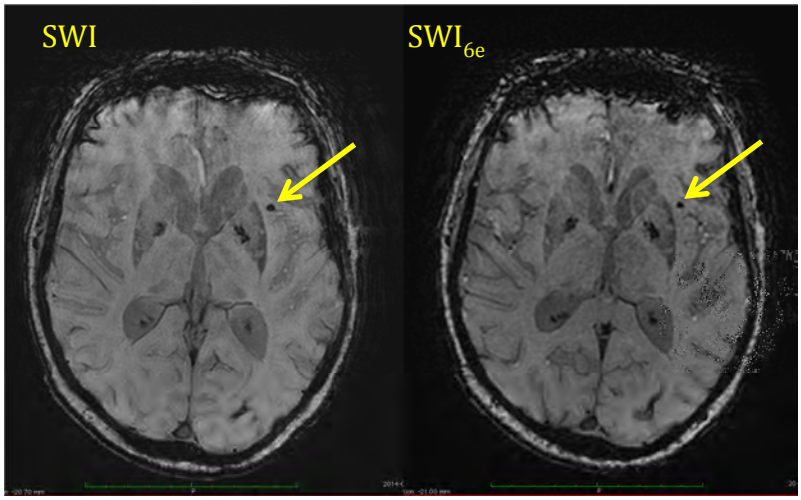

Figure 1. Example images from SWI and SWI_{6e} derived from the sixth echo of the QSM acquisition, are shown for an individual. The arrow indicates a cerebral microbleed. The in-plane resolution is slightly lower in QSM (i.e SWI6e) compared to SWI.